Elastomeric Skin Selection for a Fluid-Filled Artificial Fingertip

Dipayon Roy, Nicholas Wettels, Gerald E. Loeb

Department of Biomedical Engineering, Viterbi School of Engineering, University of Southern California, Los Angeles, California 90089
Correspondence to: D. Roy (E-mail: dipayon@gmail.com)

ABSTRACT: Biomimetic fingertips for robots and prostheses need to combine compliant grip and tactile sensing with robustness in diverse environments. We have evaluated materials for use in a compliant, fluid-filled artificial fingertip that incorporates multimodal sensing of contact, texture and thermal properties. A variety of silicone elastomers were tested for hardness, wear-rate, and stress–strain relationships. Diffusion rates of several aqueous and nonaqueous solvents through elastomeric membranes were analyzed to ensure that the sensor could maintain proper fluid volume and function for an extended period. A solution of sodium bromide in poly(ethylene glycol)-200 and water combined with a Silastic S silicone elastomeric cosmesis produced a stable and robust solution. © 2012 Wiley Periodicals, Inc. J. Appl. Polym. Sci. 000: 000–000, 2012

INTRODUCTION

Elastomers are useful in a wide variety of applications due to their compliant nature, their resistance to temperature changes, mechanical toughness and, in some cases, "self-healing" properties.[1] The benefits of compliant end effectors are readily apparent for robotic manipulators, as they aid in grip by conforming to the surfaces of contacted objects and increasing the available area to distribute loads and friction forces, much like human fingertips.[2] For dexterous manipulation, it is highly beneficial to sensorize the tips of compliant end-effectors. However, mounting tactile sensors on or in end-effectors with compliant surfaces presents many challenges. Arrays of delicate sensors are difficult to mount on curved, deformable surfaces and their electrical connections are subject to stress fatigue. Sensors placed under protective skins may be degraded by temporal and spatial low-pass filtering effects. These problems have been addressed by a multimodal fingertip sensor that uses the deformation of an elastomeric skin and underlying fluid layer as the basis for transduction.[3,4] To commercialize this technology (now known as the BioTac® from SynTouch LLC), we undertook systematic investigation into the requirements and material properties described herein. The importance of similar investigations into material selection is further illustrated by the efforts of other groups.[5]

Fluid-based tactile sensing in manipulation is not a new concept. Brockett discussed several advantages of robotic manipulanda with fluid-backed surfaces.[6] Shimoga and Gold- berg provided a comparative analysis of construction materials, including soft ones, for robotic fingertips.[7] Hristu also discussed the advantages of compliant manipulators and simultaneously proposed an optically read gel-filled sensor[8] that had some problems with ambient light. Helsel fabricated a one-dimensional impedance tomographer based on changes in fluid impedance,[9] and Russel crafted a uni-axial sensor using similar technology.[10] Electrorheological sensors[11,12] also use capacitive sensing in conjunction with an electroactive gel to combine sensing with grip stabilization. In general, these approaches have had problems with complexity and robustness in the often-hostile environments in which hands and grippers need to be used.[13–17]

In this article, we consider the BioTac® (Figure 1), whose nonlinear but wide dynamic ranges of multimodal sensing (Table I) have been described[3,18,19] (see also http://www.syntouchllc.com). Multimodal sensors facilitate the precise control of exploratory movements that is required to be able to extract the properties of objects from the sensor data.[20] For example, information about the material composition of an object can be inferred from the rate of heat transfer from a heated finger to the object, but only if the location and force of contact are well-controlled and known.[18] Similarly, information about surface textures can be extracted from the microvibrations induced in the skin and incompressible fluid, but only if the location and force of contact are well-controlled and known.[21] The deformable skin of the BioTac is intended to provide mechanical and thermal
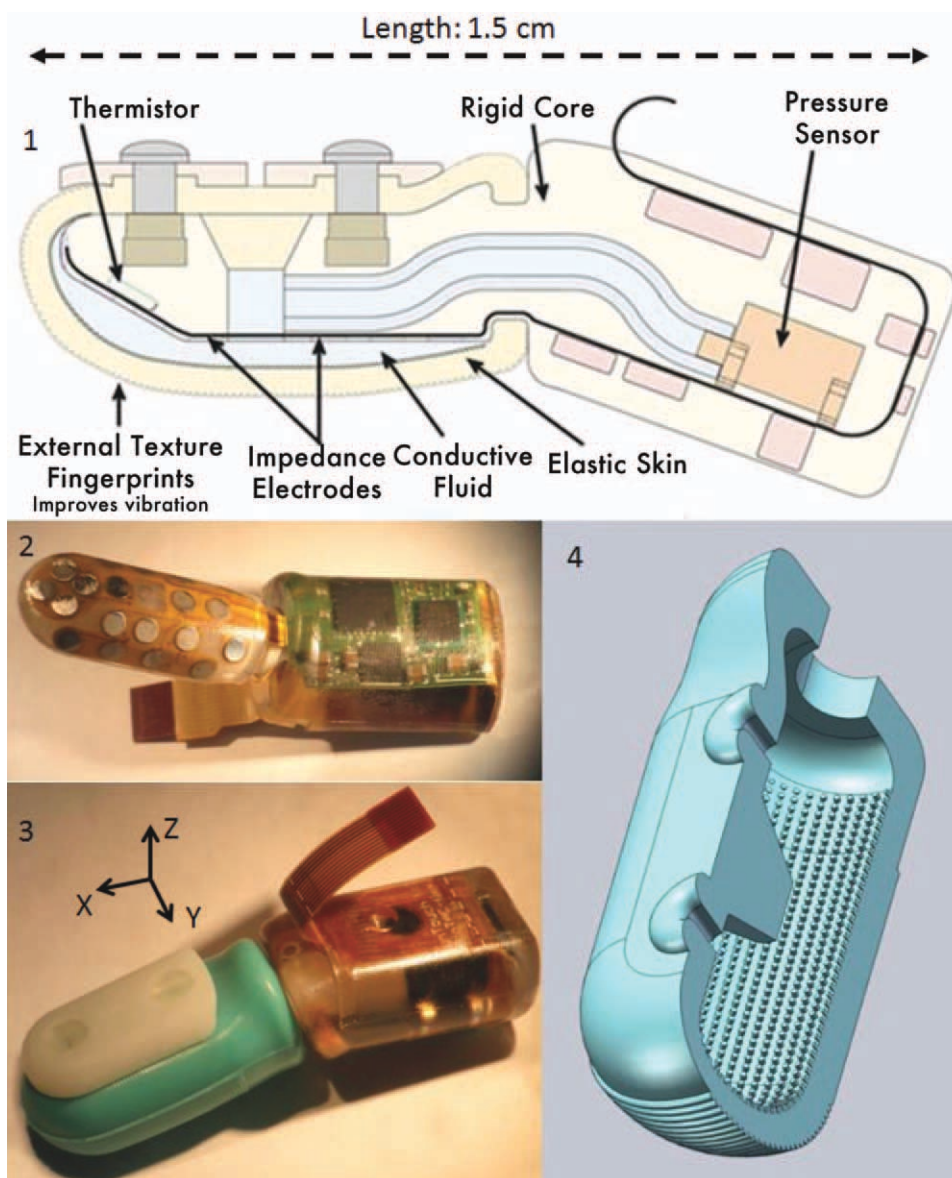
Figure 1. Lateral cross-sectional drawing of BioTac showing various components used for each sensing modality. 2: Lateral photograph of device with skin removed. Large disks on the distal portion are platinum electrodes. 3: Angular view of sensor with skin and nail installed. 4: Angular cross-sectional view of skin. [Color figure can be viewed in the online issue, which is available at wileyonlinelibrary.com.]

properties that are similar to those of the human fingertip, so material selection is an important part of its design.

A key requirement for the contact-sensing modality of the Bio-Tac is a low-viscosity, electrically conductive liquid contained within the elastomeric skin, whose deformation is sensed as impedance changes via multiple electrodes on the surface of the

Table I. BioTac Sensor Performance Characteristics

Modality	Range	Frequency response (Hz)
Force	0.01–50 N	0–50
Microvibration	0–2.0 kPa	0–2000
Thermal flux	0–1.0 C/s	0.1–50

rigid core of the fingertip. The skin must be readily deformable, resist cuts and abrasive wear, and prevent leakage, diffusion losses, and chemical interactions between the fluid and elastomer. The BioTac is intended for use in a wide range of environments where it may be subjected to wide swings in humidity and temperature. The mechanically detailed skins are designed to be replaced at regular intervals, so they must be produced from low-cost materials and manufacturing processes.

The most relevant material properties tested in this particular artificial fingertip are listed below, along with the rationale for their importance.

1. Elastomer Wear: Defined as the propensity for the elastomer to degrade mechanically and wear away with use. Although the skin of the sensor is meant to be easily

replaceable, low wear rates increase the life span of each skin. The external surface of the skin is molded with a fingerprint-like texture that greatly increases the vibrations sensed for texture and slip detection[4] but is particularly prone to wear.

2. Stress relaxation: The likeliness of an elastomeric substance to relax when put under constant stress, which may be increased by absorption of fluids. When the skin is replaced, the BioTac is inflated to the desired pressure with a small volume of the conductive fluid. Thus, the effect on the chosen elastomer of continuous contact with candidate fluids was investigated.

3. Diffusion: Because silicone elastomers are permeable to some fluids, it is important to investigate what fluids would diffuse through which elastomers and at what rate. This is part of the consideration of skin thickness, which is impacted also by the wear rate and the desired dynamic range and spatial sensitivity of contact force sensing.

4. Fluid properties: Contact force transduction in the BioTac is based on measuring changes in the conductance between electrodes through the fluid; conductivity between 100 and 1000 Ω cm is required to achieve the desired dynamic range without excessive electrical noise. This precludes the use of nonpolar fluids that have low vapor pressures and diffusion rates but are essentially nonconductive. Previous studies have also demonstrated the importance of high lubricity of the fluid to avoid hysteresis under high contact forces.[3] Low viscosity is also desirable to avoid damping the frequency response to rapid force changes and vibration.

We report here on a series of experiments that were conducted to investigate the relevant properties of various candidate elastomers and aqueous vs. nonaqueous conductive fluids. These data provide guidance for the design of the BioTac product as well as general information for the design of compliant and/or fluid-filled gripping surfaces.

ELASTOMER WEAR

Methods

The choice of elastomer is a complex topic that is closely linked to many other decisions such as fluid type as discussed below. Table II provides a list of the candidate elastomers that we considered and their most relevant mechanical properties in comparison to human skin.

The tensile strength and elongation at break of the elastomer should be high enough such that it can withstand the stretch and abrasion due to regular grip forces encountered in object manipulation and exploration. The literature supports the notion that in polymers:

$$\frac{V}{S} \propto \frac{1}{H} \times F \times \frac{1}{se} \qquad (1)$$

where V/S is the volume removed per sliding distance, H is the hardness, F is the frictional force, s is the rupture stress, and e is the strain at rupture.[23] Hardness is limited by the desired mechanical properties of the molded skin, so we hypothesized that it would be useful to select materials with high tensile strength and elongation at break, corresponding to s and e in eq. (1).

Table II. Elastomer Properties Tested Over Various Experiments

Elastomer	Type	Shore A hardness	Tensile strength (kPa)	Elongation at break (%)
Human Skin[22]	Biological	20	50–300	35–115
EcoFlex-00–10	Silicone	00–10	827	800
Dragonskin-10	Silicone	10	3275	1000
Silastic S	Silicone	26	6894	900
Silastic E	Silicone	35	5516	350
VytaFlex-10	Urethane	10	1379	1000
VytaFlex-40	Urethane	40	3599	660
VytaFlex-50	Urethane	50	4054	400
VytaFlex-60	Urethane	60	6067	480
PMC-744	Urethane	44	2068	400

Preliminary evaluation for wear was conducted by using a method similar to ASTM D1630 - 06 (Standard Test Method for Rubber Property-Abrasion Resistance). Mechanical wear can be broken down in frictional and fatigue wear. At small normal loads over longer periods of time, an elastomer generally experiences fatigue wear: dimples and pitting marks can be seen on its surface. Continually abrading an elastomer leads to chain scission, or the breaking of a group of molecular bonds. This breakage leads to the surface of the rubber rupturing in groups, rather than as a steady loss of layers. Because of this phenomenon, the surface of an elastomer has different properties than the bulk, making it difficult make accurate predictions of wear.[24]

Five urethanes and four silicone elastomers of varying hardness, tensile strength and elongation at break were tested. Each of the samples was cured overnight in a room with 26 ± 3C temp and 35 ± 12% humidity. Each material was cured in a 1" cube wax mold that produced a working surface with a 1" radius of curvature with fingerprint texture (1 mm hemispherical ridges, 1 mm edge-to-edge spacing). A JVC AL-A155 turntable with a circular surface of 220-grit sandpaper used as the abrader; the turntable was run at 60 cm/s. The rubber sample was attached to the end of the arm and a 50 g weight placed on the arm to keep constant 0.39 N force on the sample (the weight was not at the end of the arm). The turntable was run for 50 revolution increments and the rubber sample was weighed. After 350 total revolutions, the sample was run on the turntable for 2 h. The surface was periodically cleaned away using an air duster. The final mass of the rubber was documented and pictures were taken through a dissecting scope.

Results

A summary of the tested elastomers is shown in Table III along with their initial mass loss-rate after 50 revolutions; the number of revolutions at which greater than 50% of the fingerprints had worn away by visual inspection and the average mass loss-rate for the entire test.

To determine which elastomer properties lead to the least wear, it would have been most sensible to test elastomers that only varied along one single property amongst hardness, tensile strength, and elongation at break. This was not practical,

Table III. Summary of Elastomer Wear Data

Material	Initial mass loss rate (μg/rev)	Print loss (revolutions)	Average mass loss-rate (mg/min)
VytaFlex40	240	50	10.2
PMC 744	120	50	8.23
VytaFlex 10	40.0	150	1.47
VytaFlex 50	93.3	200	0.99
Silastic E	114	150	0.89
Vytaflex 60	60.6	150	0.79
Ecoflex 00-10	80.0	250	0.48
Dragonskin	73.3	300	0.27
Silastic S	80.0	>350	0.21

Table IV. Mass Loss Rate of Selected Elastomers of Similar Hardness

Product	Hardness (Shore A)	Tensile strength (kPa)	Elongation at break %	Avg. mass loss/rev (×1 mg/ rev)
VytaFlex40	40	3599	660	10.17
Silastic E	37	5516	350	0.89
Dragon Skin	10	3275	1000	0.27
VytaFlex10	10	1103	1000	1.47

however, due to commercial availability. To calculate which property (e.g., tensile strength) had the dominant effect on wear, a Spearman correlation test was performed against the average mass loss-rates. Because the materials typically varied across multiple properties, this test will only show which property is dominant. The most dominant property was elongation at break ($\rho = -0.293$), followed by tensile strength, with hardness showing the least dominance. The elastomers with the lowest wear rates had either high elongation at break or high tensile strength and/or hardness. The dominant relationship between high tensile strength and elongation at break and low wear rate becomes more obvious in Figure 2. Silastic S has the highest tensile strength and elongation at break (although only a shore A hardness of 26) and it had the lowest mass loss-rate of any elastomer tested.

To further highlight the importance of tensile strength and elongation at break, Table IV compares wear properties of pairs of elastomers with similar hardness. In the case of the Silastic E vs. VytaFlex40, it appears the increase in tensile strength leads to a much higher reduction in wear rate versus the loss in elongation at break. This also follows from the comparison between
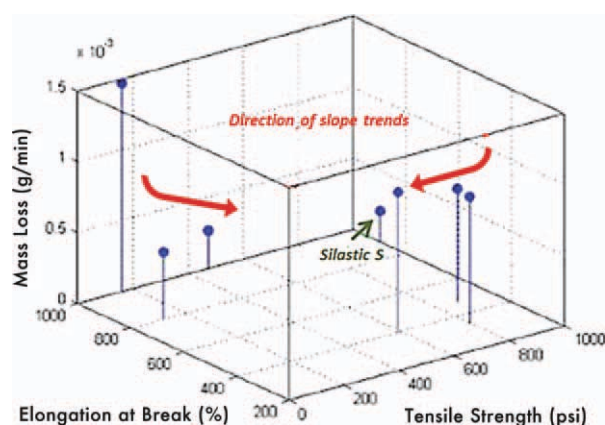
Dragon Skin and VytaFlex 10, where tensile strength is the only factor increased.

Discussion

Increasing the hardness of a material generally increases its resistance to abrasive wear by making it more likely that it will be harder than the materials with which it comes into contact. This strategy is not feasible for fingertips that must be limited to 5–50 Shore A hardness to provide sufficient compliance for good grip. Instead, tensile strength and elongation-at-break should be maximized to reduce wear by allowing the skin to strain without breaking and then bounce over the contacting surface when tangential force exceeds normal force divided by the coefficient of friction. Dow Corning Silastic S presents a good, commercially available choice, as it combines high tensile strength (1000 psi) and elongation at break (900%) and low wear rate (210 μg/min in our test) with low hardness (Shore A 26), which facilitates deformation on contact for both grip and sensing. Moreover, as a silicone elastomer, Silastic S is relatively resistant to creep during the compressive stresses to which the BioTac will be subjected when gripping objects.[25]

ELASTOMER SWELLING AND STRESS RELAXATION

Methods

Stress relaxation is the tendency of a material to relieve stresses under a constant strain by deforming; creep is similar but refers to the tendency of a material to relieve strain permanently under the influence of stresses. It is desirable to minimize both for the tactile sensing application. The rate of this deformation is a function of the material properties, exposure time, exposure temperature and the applied structural load. The effect of increasing molecular weight tends to promote secondary bonding between polymer chains and thus make the polymer more creep resistant.[26] Silicones were thus favored as an elastomer choice because, relative to other commercially available elastomers, they show little creep, little stress relaxation and thus low hysteresis. If any nonlinearity such as hysteresis is beneficial in a control application, it can always be added to the control loop software, while maintaining the reproducibility of sensor performance.

In earlier pilot experiments we noted that there was a rapid drop in internal pressure after BioTac inflation. One hypothesis for this substantial drop in pressure was the relaxation of the elastomer under the stress of fluid pressure. Another possibility was that the fluid was being absorbed into the elastomeric skin and potentially altering its mechanical properties. To evaluate this, test specimens of Silastic S (Figure 3) were submerged in
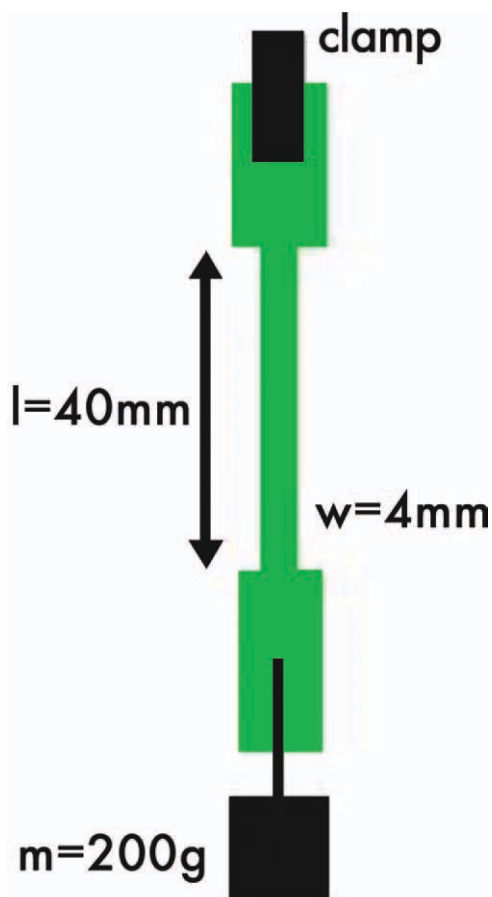

Figure 2. Plot of mass loss versus elongation at break and tensile strength (two trials removed for clarity). [Color figure can be viewed in the online issue, which is available at wileyonlinelibrary.com.]

Figure 3. Test set-up with ~ 1 g silastic *S* samples. [Color figure can be viewed in the online issue, which is available at wileyonlinelibrary.com.]

50 mL each of the following fluids: water, 1,2-propanediol, 1,2,3-propanetriol, and poly(ethylene glycol)-400 for 28 days (three specimens per fluid). Mass was measured approximately every three days after blotting dry to track changes. Every seven days, stress testing was performed on each of the strips by hanging a weight from the end. Average tensile stresses of 0.3 N/mm^2 were applied causing 140–150% elongation. Original length, stressed length, and post-stress length were measured after ~ 30 s application of stress.

A Spearman correlation was performed between the changes in % post-stressed length and the % mass gain to inspect influence on fluid absorption on stress relaxation. Spearman correlation was chosen because of the small sample size of the stress measurements ($n = 12$) and the ability of Spearman correlations to represent any monotonic, potentially nonlinear correlation.

Results

Only the samples soaked in water experienced an appreciable increase in resting length (Figure 4) and mass (Figure 5). This relationship is further highlighted in Figure 6, where post-stress % length change and mass change are plotted together. Only water-soaking yielded a marginally significant Spearman correlation coefficient (0.357, $P < 0.128$, single-tail).

Discussion

The results show that water is not only able to absorb into the Silastic, but that it also has an effect on its mechanical properties, suggesting that it not a good fluid base. Avoiding exposure to water or water vapor in any application for the BioTac is nearly impossible, which emphasizes the importance of a nonaqueous fluid base. However, due to the hygroscopic nature of all of the candidate nonaqueous solvents, a low concentration of
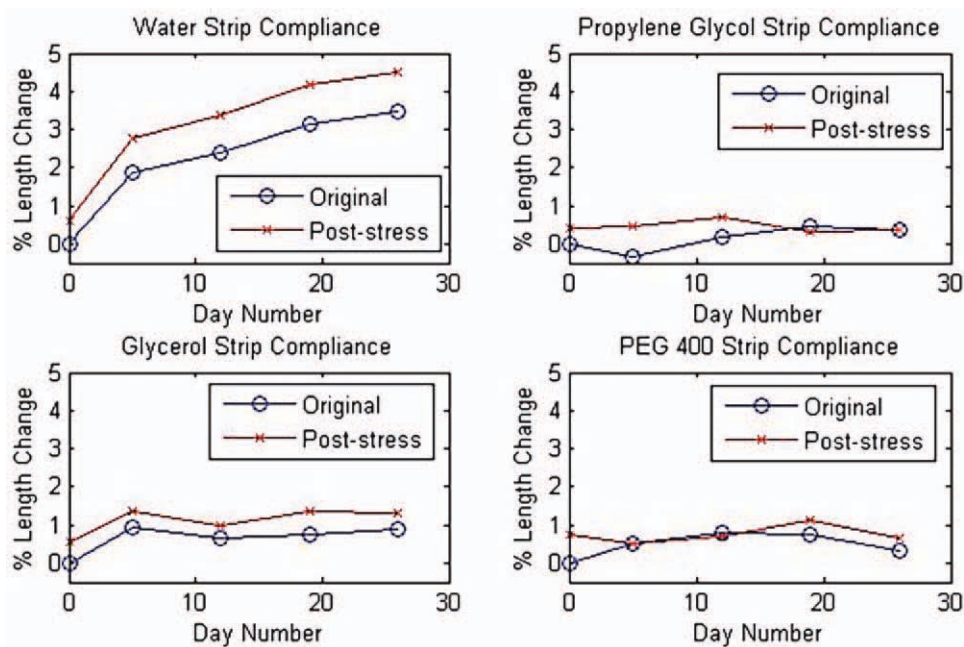

Figure 4. Percentage length change of silastic *S* test samples in over time soaking in four different liquids (data points averaged for three samples for each test condition); blue circles = original or prestressed length, red X = post-stressed. The stressed lengths for each sample did not vary substantially over the 4-week test period. [Color figure can be viewed in the online issue, which is available at wileyonlinelibrary.com.]
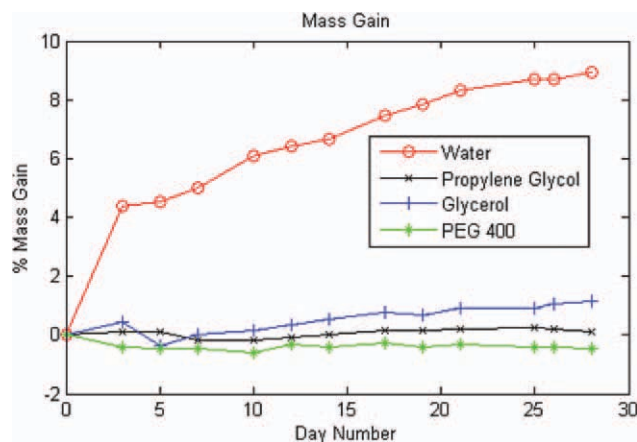
Figure 5. Percentage change in sample mass (averaged over three samples). [Color figure can be viewed in the online issue, which is available at wileyonlinelibrary.com.]

water is likely to help in regulating conductivity and diffusion of water in and out of the sensor based on the relative humidity of the environment. These concentrations of water are discussed in more detail in Table VI in Section IV.

DIFFUSION

Methods

Perhaps the most important consideration for this sensor is diffusion of fluid through the elastomeric membrane. It is important to choose an elastomer with a low enough diffusion coefficient such that negligible or manageable fluid loss occurs over the service life of the cosmesis (typically 4–6 months in prosthetic limbs). Diffusion will vary depending upon thickness of elastomeric membrane, temperature, size and shape of the molecule of the solvent, salt content of fluid, hygroscopicity, environmental humidity, and polar properties of solvent and membrane. The internal pressure of the device will also drive fluid loss. Because of the highly desirable mechanical properties of the silicone elastomer chosen above, we focused on systematic comparisons of candidate fluids and their properties as outlined in Table V. Preliminary experiments suggested that inward and outward diffusion of water was the most important factor. Net volume change would then depend on the hygroscopicity of the fluid and the ambient humidity, which were varied systematically in the studies presented here.

Net fluid diffusion coefficients were determined for two candidate silicones, one urethane skin, and various fluid combinations (see Table VII in Results). All of the fluids had the required salt solubility and conductance, high lubricity and low viscosity. Thin, large surface area skins were molded over aluminum rods, cured, peeled from the rods, and filled with test fluid. The skin/fluid sacs were plugged with a small disc of aluminum rod and resealed with their respective elastomers. To evaluate also the in-flux of water from the environment and the potential hygroscopic properties of the fluids, one batch of test samples was kept in a humidifier (Styrofoam container with a damp sponge). Weighing occurred at 24-h intervals over 10 days to monitor mass changes in the samples. The net outward diffusion coefficients were calculated using data from the desiccated samples to minimize effects
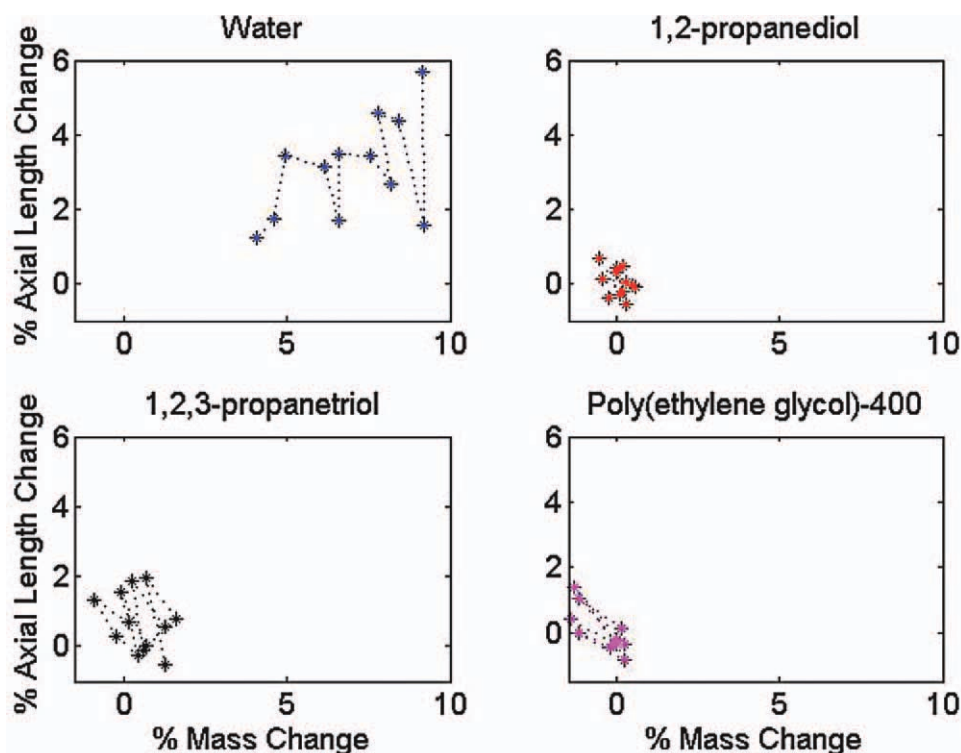

Figure 6. Percentage mass change versus percentage sample length change. [Color figure can be viewed in the online issue, which is available at wileyonlinelibrary.com.]

Table V. Fluids Tested Over Various Experiments (All Relevant Values at STP)

Fluid	Density	Molecular weight	Frz. Pt (°C)	Boiling Pt	Viscosity	Vapor pressure	Formula
Water	1.00 g/cm^3	18	0	100	1 cP	23.76 mmHg	H_2O
1,2-Propanediol	1.04 g/cm^3	76.09	−59	188	54 cP	0.08 mmHg	$C_3H_8O_2$
Poly(ethylene glycol)−200	1.12 g/cm^3	190–210	−65	250	50 cP	<0.01 mmHg	$HO(C_2H_4O)_nH$
Poly(ethylene glycol)−400	1.12 g/cm^3	380–420	5	250	90 cP	<0.01 mmHg	$HO(C_2H_4O)_nH$

of humidity. The coefficients were calculated by using Mass Flux and Fick's First Laws[27]:

$$J = \left(\frac{1}{A}\right) \cdot \left(\frac{\Delta M}{\Delta t}\right) \qquad (2)$$

where A = total surface area, ΔM= change in mass and Δt = change in time (Mass Flux).

$$J = -D \cdot \frac{\Delta C}{\Delta x} \qquad (3)$$

where D = Diffusion coefficient, ΔC = change in concentration (density of fluid in this case), and Δx = thickness of skin (Fick's First Law). The first order ordinary differential equation can be solved to generate a model for how fluid will diffuse out of the skin over given time [eq. (4)].

$$M = M_0 e^{-\frac{DA}{V_x} t} \qquad (4)$$

Diffusion can be affected by multiple factors, including temperature and any physical gradient caused by pressure or a concentration differential or both. Because the fluid inside the BioTac is pressurized, a driving head is added to the diffusion of the fluid across the membrane. Furthermore, relative humidity will affect the internal pressure of the sensor as more water diffuses in or out based on atmospheric water vapor content. Changes in gradient pressure would be minimal for the large volume-to-surface-area of the diffusion test skins, but it was necessary to validate these findings for the actual BioTac, which has a much smaller volume-to-surface-area but a much thicker skin.

In the validation, three BioTac sensors were used. Each BioTac was inflated with NaBr solutions based on water, 1,2-propanediol with 18% water, or poly(ethylene glycol)-400 mixed with 8% water (see footnote to Table VI). These solutions were based

Table VI. Fluid Composition in Each Test BioTac

	BioTac 1	BioTac 2	BioTac 3
Molarity (NaBr)	0.68M	1.0M	1.0M
% Water (bv)	8%	18%	100%
Nonaqueous base	Poly(ethylene glycol)−400	1,2-Propanediol	None

Water content based on experimentally determined hygroscopicity of respective nonaqueous base.

on preliminary investigations, which suggested that they would be fairly close to a balance of inward (hygroscopic) and outward diffusion of water in a typical ambient of ∼ 40% relative humidity. Approximately 250 μL were injected into the BioTac, which was enough to cause a pressure of 3.5–4.0 psi, which we determined separately produced optimal sensitivity for normal forces.[28] The sensors were then placed first in an ambient environment (∼ 40% RH) for 2 days, an arid environment (<5% RH) for 7 days, then in a humid environment (>95% RH) for 7 days, and finally in an ambient environment (∼ 40% RH) for another 7 days.

Because silicone elastomers have a high diffusion rate for water, we expected that most of the water would diffuse from all of these solutions in an arid environment. Most of any remaining fluid and salt should then stay in the sensor. We expected that the relatively small 1,2-propanediol molecule would diffuse faster than the larger poly(ethylene glycol)-400 polymer, whose diffusion rate would be negligible. When placed in a humid environment, the water would diffuse back in according to the hygroscopicity of the remaining fluid, returning the fluid volume to its original level or even beyond.

The weight of the BioTac, the relative humidity, and the temperature were recorded daily. Pressure data and electrode impedance were recorded through a custom LabVIEW program, which sampled once per minute. Preliminary experiments suggested that the electrode impedance values would not change much because the reciprocal changes in thickness of the fluid

Table VII. Diffusion Results for Various Elastomer-Solvent Combinations

Elastomer	Fluid	Diffusion coefficient (×10^{-9} cm^2/s)
Dragonskin silicone	Water	3.88
Silastic E silicone	1,2-Propanediol	0.891
Silastic E silicone	Poly(ethylene glycol)−200	2.04
Silastic E silicone	Poly(ethylene glycol)−400	0.263
PMC-744 urethane	Water	8.51
PMC-744 urethane	1,2-Propanediol	6.68
PMC-744 urethane	Poly(ethylene glycol)−200	6.21
PMC-744 urethane	Poly(ethylene glycol)−400	5.00
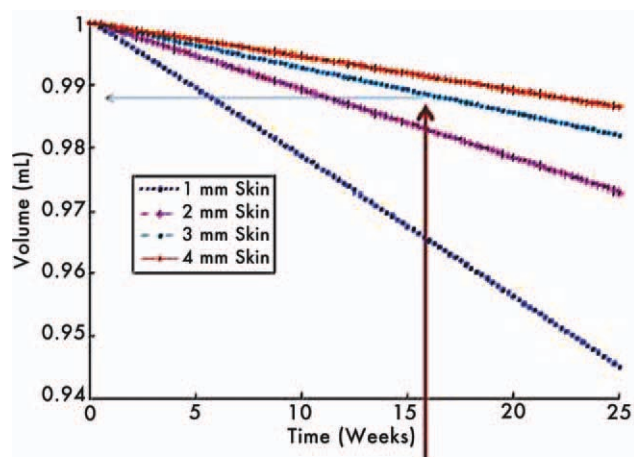
Figure 7. Hypothetical fluid migration volumes for BioTac sensor with Silastic *E* skin and 1,2-propanediol. This model assumes no pressure inside the sensor. [Color figure can be viewed in the online issue, which is available at wileyonlinelibrary.com.]

layer and salt concentration tend to compensate for each other as water content fluctuates. Finally, because the epoxy (Stycast 1264) is known to absorb moisture, a separate validation was also conducted to quantify the amount of water absorbed by the epoxy used in the core of the BioTac.

This preliminary experiment showed that the amount of moisture absorbed by the epoxy in a BioTac without fluid would be equivalent to approximately 16% of the mass of fluid used to inflate the BioTac. In an arid environment, a similar amount of moisture is released by the epoxy. Thus, the mass of an inflated sensor could potentially decrease by more than the mass of the water contained in the fluid. Given the epoxy's absorption and release of moisture, diffusion of the non-aqueous base itself would not be a concern unless the mass loss was greater than the sum of both the mass of the water in the fluid and the additional 16% that would be released by the epoxy.

Results

Each of the solvent–elastomer combinations and their respective diffusion coefficients are presented below in Table VII. The dry environment was maintained at a relative humidity of 19.6 ± 5.3% and a temperature of 25.2 C ± 0.4°C. The damp environment was maintained at a relative humidity of 79.8 ± 3.1% and a temperature of 25.6 C ± 0.5°C.

If we apply the mass-diffusion solution to the BioTac geometry (~ 6 cm^2 surface area) for Silastic E elastomer with 1,2-propanediol solution at various thicknesses, we predict that the diffusion rate is manageable (Figure 7).

In the actual BioTac sensors (Figure 8), the pressure dropped when placed in an arid environment due to a loss in water mass. The mass of each increased when placed in the humid environment, and the mass decreased at a low rate when placed in the ambient environment.
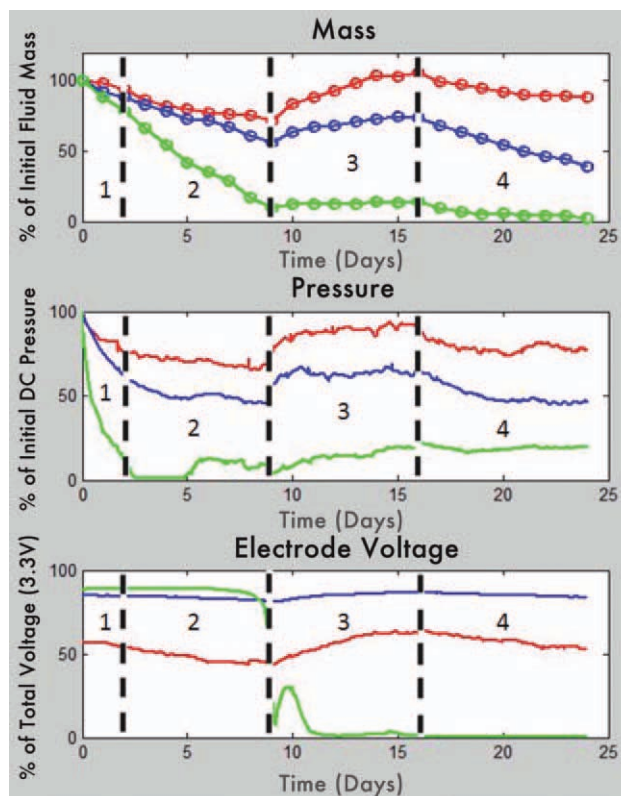

Figure 8. Percentage initial fluid mass, pressure, $V_{Electrode}$ over the 24-day trial period. The red trace (highest trace at Day 24 in "Mass" & "Pressure," middle trace at Day 24 in "Electrode Voltage") refers to the poly(ethylene glycol)-400 and water solution (BioTac 1 in Table VI), the blue trace (middle trace at Day 24 in "Mass" & "Pressure," highest trace at Day 24 in "Electrode Voltage") refers to the 1,2-propanediol and water solution (BioTac 2), and the green trace (lowest trace at Day 24 in "Mass," "Pressure," & "Electrode Voltage") refers to the water-only solution (BioTac 3). The vertical dotted lines indicate a change in environment according to Table VIII, where "1" is ambient, "2" is arid, "3" is humid, and "4" is ambient. Temperature did not vary significantly over the course of the experiment. (Mass recorded every 24 h; pressure and electrode voltage sampled at 0.017 Hz). Electrode voltage readings failed for the water-only solution at day 9, as discussed below. [Color figure can be viewed in the online issue, which is available at wileyonlinelibrary.com.]

Discussion

On the basis of the results from the fluid sac experiment, if the unit is not under pressure, both PG and PEG-400 in conjunction with a 2- to 3-mm-thick Silastic E cosmesis would function as a nondiffusive unit over the life of the device. Even if the

Table VIII. Environment Changes for Each BioTac*

	Period 1	Period 2	Period 3	Period 4
Environment	Ambient	Arid	Humid	Ambient
Duration	2 days	7 days	7 days	7 days
Relative humidity	40%	<5%	>95%	~ 40%

*BioTac 1: 0.68M NaBr in water, 8% by volume in poly(ethylene glycol)−400; BioTac 2: 1.0M NaBr in water, 18% by volume in 1,2-propanediol; BioTac 3: 1.0M NaBr in water only.

predictions of the model were inaccurate by a large amount, the device could easily be refilled by a minimally skilled technician. Regarding further fluid and elastomer choices, poly(ethylene glycol)-400 is preferred over 1,2-propanediol due to the lower diffusion coefficient, higher hygroscopicity, and similar lubricating properties. Given the similar chemistry of the Silastic series, similar results are expected for Silastic *E* and *S*.

The results from the experiment that use actual inflated and pressurized BioTac sensors help explain why poly(ethylene glycol)-400 is a better choice than the smaller 1,2-propanediol. Pressure can act as an accelerant for diffusion of molecules that would not diffuse through a membrane such as the BioTac skin when there is no pressure gradient. While the trends are similar in the case of each fluid, it is the relative magnitude of the trends that is most important in choosing the appropriate fluid. In the 1,2-propanediol solutions, the outward diffusion of both water and 1,2-propanediol was only partially compensated by the inward diffusion of water in the humid environment. For the poly(ethylene glycol) solution, however, the inward diffusion of water back into the sensor compensated almost completely for the initial water loss. While the poly(ethylene glycol)-400 only contained 8% water, the mass loss in the arid environment was ∼ 25%. The additional mass loss can be explained by the release of moisture by the epoxy rather than diffusion or other leakage of the poly(ethylene glycol). This is confirmed by the stabilization of pressure in BioTac after an initial change due to the efflux of water. In the BioTac with the 1,2-propanediol solution, there is greater than a 45% decrease in mass in the environment, which is substantially greater than the maximal possible loss of 34% from water in the fluid (18%) plus moisture from the epoxy (16%). Thus, while the 1,2-propanediol did not seem to diffuse out in appreciable quantities when tested in the unpressurized fluid sacs, the addition of a pressure gradient appears to cause a significant amount of diffusion of the 1,2-propanediol itself, which in turn reduces the stability of the BioTac's DC Pressure and robustness.

The results for the water-based fluid in the sensor (Figure 8) confirm the predictions of the diffusion experiment. Silicone elastomers are generally highly permeable to water, so much of the fluid volume was rapidly lost. By day 9, enough fluid had diffused out to interrupt the sensor's ability to function (explaining the drop in the green trace). In contrast, the poly(-ethylene glycol) solution maintained pressure, mass, and conductivity; the 1,2-propanediol solution's behavior was intermediate, as it was able to maintain fluid conductance despite losing significant mass through diffusion.

Close examination of the Electrode Voltage plot in Figure 8 reveals that there is a noticeable increase in conductivity when water diffuses into the poly(ethylene glycol)-400 in a humid environment. In subsequent development, this problem was greatly reduced by switching to poly(ethylene glycol)-200 as the nonaqueous base, which provides higher ionic mobility and can dissolve a higher salt content. The diffusive properties of poly(ethylene glycol)-200 are similar to those of poly(ethylene glycol)-400 based on their similar physical structure, as each molecule is a polymer with an ethylene glycol backbone. Previous tests had suggested that poly(ethylene glycol)-200 is more hy-

groscopic than poly(ethylene glycol)-400, so the water content was increased accordingly to maintain equilibrium. The molarity was also increased to $0.9M$, which lowers resistivity to 851 Ω cm compared with 1640 Ω cm for the $0.68M$ poly(ethylene glycol)-400 solution. The resistivity of this solution is much less affected by small changes in water concentration in the fluid.

CONCLUSIONS

The final choice of fluid for the BioTac sensor is a mixture of $0.9M$ NaBr in water, 12% by volume in poly(ethylene glycol)-200. This solution combines desirable diffusion, lubrication, hygroscopicity, and conductivity properties. Although these values vary somewhat for various durations of exposure to varying environmental conditions, they do so slowly and in a way that is nondestructive to the operation of the sensor. These slow changes can be compensated by implementing zeroing or calibration algorithms that occur quickly relative to the rate of the environmental effects, similar to "taring" a scale before weighing a sample. Similar calibration presumably occurs in the neural processing of tactile signals from human fingertips, whose mechanical properties are also affected by temperature, humidity, wear, and regeneration. The desire to balance function and robustness in an engineered system inevitably requires compromises in various parameters such as skin thickness and hardness and fluid conductivity.

REFERENCES

1. Keller, M.; White, S.; Sottos, N. *Adv. Funct. Mater.* **2007,** *17,* 2399.
2. Son, J. S.; Howe, R. D. Proceedings of the IEEE International Conference on Robotics and Automation, Minneapolis, April 22–28, **1996,** p 3228.
3. Wettels, N.; Santos, V. J.; Johansson, R. S.; Loeb, G. E. *Adv. Robotics* **2008,** *22,* 7.
4. Fishel, J. A.; Santos, V. J.; Loeb, G. E. Proc. IEEE Intl Conf Biomed Robotics and Biomechatronics (BioRob), December 7, **2008,** Paris.
5. Berselli, G; Piccinini, M.; Palli, G.; Vassura, G. *IEEE Trans Robotics* **2011,** *27,* 3.
6. Brockett, R.W. Proceedings of the IEEE Conference on Robotics and Automaton, Philadelphia, PA, **1985,** p 942.
7. Shimoga, K. B.; Goldenberg, A. A. *Int. J. Robotics Res.* **1996,** *15,* 320.
8. Hristu, D.; Ferrier N.; Brockett, R. W. Proc of the IEEE International Conference on Robotics & Automation San Francisco, CA, **2000.**
9. Helsel, M.; Zemel, J. N.; Dominko, V. *Sens Actuators* **1988,** *14*:1, 93.

Applied Polymer
SCIENCE

10. Russell, R. A.; Parkinson, S. Proceedings of IEEE International Conference on Robotics and Automation Atlanta, GA, **1993**, p 423.

11. Kenaley, G.; Cutkosky, M. 1996 IEEE International Conference on Robotics and Automation, Scottsdale, AZ, **1989**, p 132.

12. Voyles, R. M.; Fedder, G.; Khosla, P. K. Proc of the IEEE International Conference on Robotics and Automation, Minneapolis, MN, **1996.**

13. Lee, M. H.; Nichols, H. R. *Mechatronics* **1999**, *9*, 1.

14. Howe, R. D. *J. Adv. Robotics* **1994**, *8*, 245.

15. Melchiorri, C. Tactile Sensing for Robotic Manipulation, in Ramsete: Lecture Notes in Control and Information Sciences; Springer: Berlin, **2001; Vol.***270.*

16. Grupen, R. A.; Henderson, T. C.; McCammon, I. D. *Int. J. Robotics Res.* **1989**, *8*, 38.

17. Dahiya, R.; Metta, G.; Valle, M.; Sandini, G. *IEEE Trans. Robotics,* **2010**, *26*, pp.

18. Wettels, N.; Fishel, J. A.; Su, Z.; Lin, C. H.; Loeb, G. E. 9th IEEE-RAS International Conference on Humanoid Robots. Tactile Sensing in Humanoids—Tactile Sensors and Beyond Workshop, Paris, France, December 7–10, **2009.**

19. Wettels, N.; Loeb, G. E. Haptic feature extraction from a biomimetic tactile sensor: force, contact location and curvature. IEEE-ROBIO, Phuket, Thailand, Dec. 7–11, **2011.**

20. Su, Z.; Fishel, J. A.; Yamamoto, T.; Loeb, G. E. *Frontiers Neurorobotics, to appear.*

21. Fishel, J. A.; Loeb, G. E. *Frontiers Neurorobotics.* 6:4. doi: 10.3389/fnbot.2012.00004.

22. Edwards, C.; Marks, R. *Clin. Dermatol.* **1995**, *13*, 375.

23. Lancaster, J. K. *Wear* **2001**, *141.1*, 159.

24. Gent, A. N.; Pulford, C. T. R. *J. Appl. Polym. Sci.* **1983**, *28*, 943.

25. Kornbluh, R.; Pelrine, R. In Dielectric Elastomers as Electromechanical Transducers; Carpi, F.; De Rossi, D.; Kornbluh, R.; Pelrine, R.; Sommer-Larsen, P., Eds.; Oxford, UK: Elsevier, **2008, 41.**

26. Meyers, M. A.; Chawla, K. K. Behavior of Materials, 2nd ed.; Prentice-Hall: New York, **1999.**

27. Calister, W. D. Fundamentals of Materials Science and Engineering, An Integrated Approach, 2nd ed.; Hoboken, NJ: Wiley, **2005;** p 158.

28. Su, Z. Unpublished, **2010.**

WILEY ONLINE LIBRARY